Interlayer coupling in Tb/Fe bilayers and Tb/Au/Fe trilayers with sharp or rough interface

E. V. Shypil, A. M. Pogorily, D. I. Podyalovski, and Y. A. Pogoryelov

Institute of Magnetism, National Academy of Sciences of Ukraine, 36-b Vernadsky Ave., Kiev 03142, Ukraine
E-mail: elena@im.imag.kiev.ua

Bilayer films Fe/Tb (Tb on Fe) having sharp and Tb/Fe (Fe on Tb) having rough interface were prepared by molecular beam epitaxy to study interlayer magnetic coupling. Magnetic properties of these bilayers were characterized *ex situ* using ferromagnetic resonance (FMR), polar magneto-optical Kerr effect and SQUID magnetometer. The resulting perpendicular magnetic anisotropy (PMA) is discussed as an effect of interlayer magnetic coupling. PMA was observed in rough as well as in sharp interfaces and the anisotropy energies were estimated. When a monolayer of Au was interposed at the interface of both kinds, PMA was observed to disappear and the overall magnetic moment increased. It was also shown that in ultrathin films demagnetization factor depends on the substrate roughness and should be considered in the FMR data.

Introduction

Coupling between ferromagnetic metal layers separated by nonmagnetic metal interlayers (first reported by Grünberg et al. [1] in Fe/Cr multilayers) was observed in many systems: Fe/Al [2], Fe/Ag [3], Fe/Au [2,4–7], Fe/Pd [8], Fe/Cu [8,9]. Indirect exchange coupling between ferromagnetic (Fe) layer and rare earth metal (Tb) separated by nonmagnetic metal interlayers (Cu, Au, Pt, Ta) was also found [10]. Authors concluded that PMA in Fe/Tb multilayers was due to a short range interaction between the nearest neighbours (Fe–Tb) at the interface. Besides this interaction, a long-range indirect exchange via a nonmagnetic metal interlayer was also observed. Though this first and the only work on Fe/M/Tb structures [10], where M is nonmagnetic metal, showed interesting results, it also put many questions. It became clear that the coupling modes need further investigation.

It is important to note that magnetic properties of amorphous rare earth–transition metal alloy films and multilayers were studied extensively in the past [11–24]. Among them Tb–Fe system that shows significant PMA and already finds application as magneto-optic data storage media, has been investigated more. Tb/Fe multilayers show better promise for this purpose compared with alloy films, and their magnetic properties have been also well investigated [16–24]. Antiferromagnetic coupling of Tb and Fe magnetic moments at the interface has been established [15,25] similar to antiferromagnetic interactions in amorphous alloys. It was also noticed that when the thickness of individual layers is small, a few monolayers (MLs), then the roughness of the interface and its effect on the interfacial magnetic interactions cannot be neglected.

As a consequence of the different atomic radii R and surface energies of Tb and Fe, the different structures for Tb grown on Fe (Fe/Tb, sharper interface) or Fe grown on Tb (Tb/Fe, rougher interface) can be expected [26]. This is schematically shown in Fig. 1. Magnetic properties of both kinds interfaces were studied regarding PMA and it was shown that the rough interface is a stronger source of PMA at room temperature than the sharp one [19–21].

However, so far, most of the studies reported on Tb/Fe even regarding rough and sharp interfaces [19–24], have been done on multilayers, that are usually characterized as follows: i) both kinds of interface, sharp and rough, are present together and it is impossible to have clear picture as to the each kind of interface; ii) some thickness spread of the
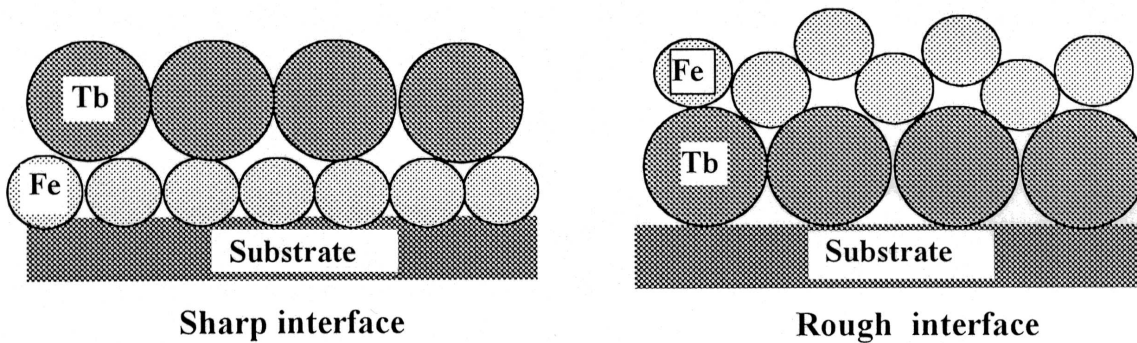
Fig. 1. Schematic picture of sharp and rough structural interfaces in Tb/Fe bilayers.

same layers is always present; iii) conclusions are done with account of the integral picture of interactions in multilayer, though it is clear that the coupling there is a sum of couplings in two kinds of interfaces plus collective interaction of all the layers in structure. All these moments make the whole picture unclear and can affect the results.

Therefore to clarify the obscure points in magnetic interactions it is necessary to investigate the *single* Tb/Fe and Fe/Tb interfaces. If to account the real thickness of the films participating in coupling, the problem can be formulated as follows: to use the modern technology for preparation of ultrathin films of high quality and to measure them with the correspondent accuracy.

The present work is undertaken to systematically study the interlayer interactions in a single Tb/Fe bilayers by carefully preparing samples under the cleanest condition with either a sharp or a rough interface. Also the effect of Au monolayer introduced at the interface is investigated.

Experimental details

Two sets of samples, Fe/Tb bilayers and Fe/Au/Tb trilayers on quartz substrate were prepared by electron-beam evaporation in an MBE system with a background pressure of $(1-5) \cdot 10^{-10}$ Torr and maintaining a pressure of $(1-3) \cdot 10^{-9}$ Torr during the film growth. To minimize interdiffusion of layers the substrate temperature during evaporation was kept no higher than 0 °C. The rates of evaporation did not exceed 0.4 Å/s and were independently controlled with quartz crystal monitors. All the samples were protected with 100 Å thick layer of Al_2O_3 .

Very small amounts of magnetic material in the present ultrathin films make it difficult for measurement. We used SQUID magnetometer, ferro-magnetic resonance (FMR) and polar magneto-optical Kerr effect (PMOKE) for characterizing the films magnetically.

SQUID (Quantum Design MPMS-5S) measurements of the films were done with the magnetic field applied either perpendicular or parallel to the sample plane and at temperatures 77 to 300 K. FMR was measured at room temperature by means of conventional modulation rf spectrometer at 9.41 GHz, with an applied magnetic field (up to 0.7 T) in the film plane. PMOKE was measured at room temperature using a 630 nm laser in an applied field up to 1.8 T perpendicular to the film plane. These measurements allowed us to infer the effect of substrate roughness and film surface on shape anisotropy.

The thicknesses of the individual layers, d_{Fe} and d_{Tb} , were chosen on the basis of our previous experiments [27–29] and literature data [10], where the ferrimagnetic ordering of Fe/Tb multilayer has been shown. This is caused by the interface properties, where ferromagnetic Fe and paramagnetic Tb being in contact, result in some magnetic moment to be induced in the Tb layer. The coupling is not restricted to the first Tb ML. It was described by «magnetic interface» of the finite volume, spread into both layers close to interface, where Fe and Tb atoms are antiparallel coupled showing PMA. The ratio of MLs, N_{Tb}/N_{Fe} , participating in the completed «magnetic interface» is usually in the range of 1 to 2, where N_{Tb} and N_{Fe} are the numbers of corresponding MLs, involved in the coupling. In this range, anisotropy energy is constant and has an approximate value $k_{\perp} \cong 5 \cdot 10^{6}$ erg/cm^3 [29]. It was also shown that the radius of pair interaction in this system is 7–15 Å [27,29]. Hence it follows that magnetic interactions in Tb/Fe interfaces begin when each of the layers, d_{Fe} and d_{Tb} , reaches 3 MLs.

Accounting that atomic radii are $R_{Fe} = 1.27$ Å and $R_{Tb} = 1.78$ Å, we choose $d_{Fe} = 8$ Å and $d_{Tb} = 12$ Å to obtain 3 MLs of Fe and 3 MLs of Tb. Samples with $d_{Tb} = 40$ Å were also prepared to study interface with the excess of Tb.

Results and discussion

Control films

Individual magnetic layers were initially studied. The hysteresis loop for 8 Å Fe film at 295 and 77 K shows good saturation as well as low coercivity with in-plane magnetization (Fig. 2,a). For 200 Å Tb and 12 Å Tb films the temperature dependence of magnetization, measured with an applied field of 250 mT are shown in Fig. 2,b. To avoid the curves distortion, substrate correction was not done. Thicker film shows the typical behavior for metallic Tb over the temperature range from 4 to 300 K — ferromagnetic below 218 K and paramagnetic above 230 K [30], whereas 12 Å Tb film shows paramagnetic behavior in the entire temperature range. Ferromagnetic resonance field was measured to be 49 mT for 200 Å Fe film, that is in good agreement with literature data of 50 mT (for the same frequency) [31,32], whereas 8 Å Fe film showed mag-netic resonance line at 150 mT. In the case of 12 Å Tb film the electron paramagnetic resonance occurred at 220 mT. These are shown in Fig. 3,a.

It is well known that FMR for an in-plane magnetized film is described by the equation

$$(\omega/\gamma)^2 = H_{\parallel} \, [H_{\parallel} + N_{eff} \, M_s - 2k_{\perp}/M_s] \qquad (1)$$

where $\omega = 2\pi f$; f is the microwave frequency; γ is the gyromagnetic ratio; $H_{\parallel}$ is the external magnetic field; M_s is the saturation magnetization; $N_{eff} = (N_{\perp} - N_{\parallel})$, where $N_{\parallel}$ and $N_{\perp}$ are demagnetization factors in plane and perpendicular to film and $k_{\perp}$ is the PMA energy. Additional condition for the demagnetization factors is $(N_{\perp} + 2N_{\parallel}) = 4\pi$. Influence of internal stresses caused by the difference in thermal expansion of the film and the substrate are accounted in the value of N_{eff}.

It is also known that for the thick Fe film $N_{\perp} = 4\pi$ and therefore $N_{\parallel} = 0$. However for ultra-thin film, when the film thickness is comparable with the substrate roughness and film becomes wavy, $N_{\perp} \neq 4\pi$. Hence, for the thinner Fe film the shape anisotropy changes comparing a perfectly flat film [33]. It has been shown that in the limit of few atomic layers the average demagnetization factor $N_{\perp}$ for a film containing n atomic layers is reduced
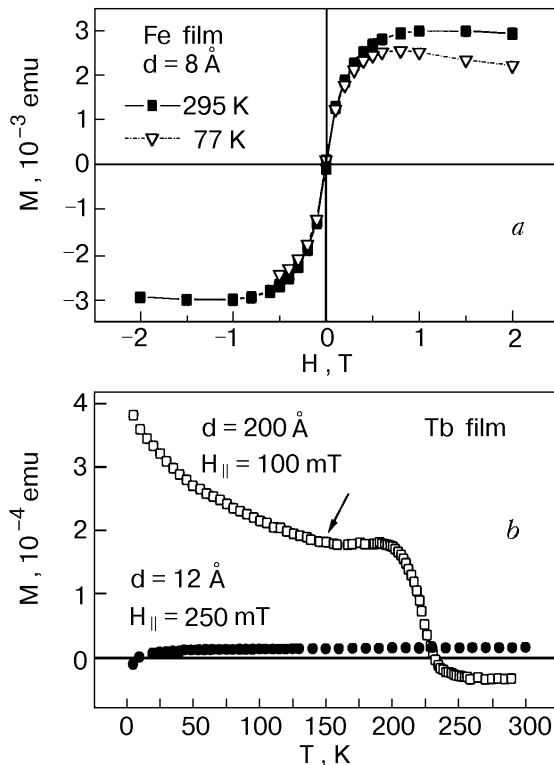
Fig. 2. Magnetization data for control films. M vs. H for 8 Å Fe (a) and M vs. T for 12 Å Tb (b) control films, measured with $H_{\parallel} = 250$ mT by SQUID. In (b) Tb film 200 Å thick is also shown.
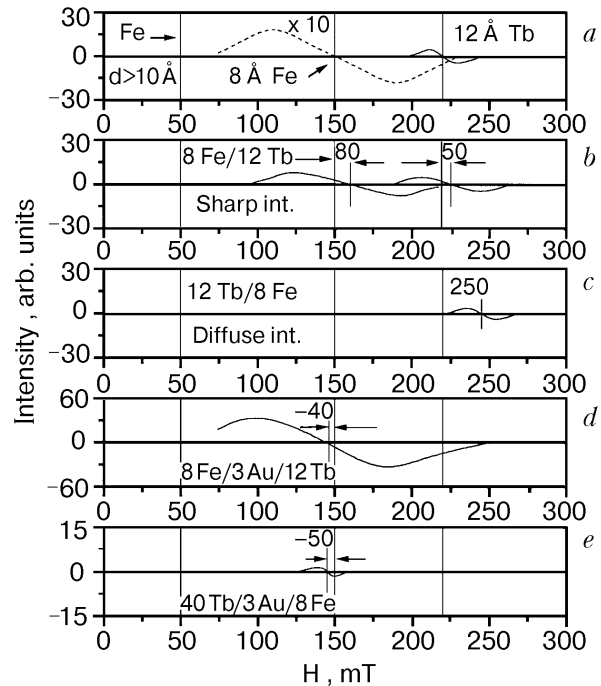
Fig. 3. FMR data for bilayers and trilayers. Positions of $H_{\parallel}$ are shown for three control films: thick Fe, thin Fe and thin Tb film (a); bilayer with sharp interface (b); bilayer with rough interface (c); trilayer with Au introduced into sharp (d) and rough (e) interfaces.

to $N_\perp = 4\pi(1 - A/n)$ (where A is a constant, having definite values for layers with different structure) [34], while the magnetization changes much slower [33]. It has also been shown by Reiger [35] that ultrathin epitaxial Fe films show the full bulk atomic magnetic moment even for the first Fe ML.

The roughness of quartz substrate used in the current work was measured by an AFM and was estimated as 5–10 Å, which is comparable to the thickness of 8 Å Fe. The FMR line for 8 Å Fe film shifted for higher H compared to the thick Fe film. This shift can be attributed to the change of demagnetization factors; $N_\perp$ and $N_\parallel$ were calculated using $M_s = 1760$ G and $H_\parallel = 150$ mT: $N_\perp = 6.56$ and $N_\parallel = 3.0$.

Coming back to magnetic properties of the control films, our above data show that 8 Å Fe film is ferromagnetic at room temperature whereas 12 Å Tb film is paramagnetic even down up to 5 K.

Bilayers–interlayer interaction at Fe/Tb *interface*

It has been shown that when thin Fe and Tb films are layered one at another, a small magnetic moment is induced in thin Tb film by Ruderman–Kittel–Kasuda–Yosida (RKKY) interaction [10,26]. Moreover, antiferromagnetic coupling of Tb and Fe magnetic moments at the interface has also been established [15,25] similar to antiferromagnetic interactions in amorphous alloys. Hence, three kinds of interactions are to be discussed in Fe/Tb interfaces: i) between Fe–Tb atoms with antiparallel orientation, which gives the main contribution to PMA. RKKY interaction is evaluated for this case as $D_{Fe-Tb} = -2.152 \cdot 10^{-14}$ erg/r^3_{Fe-Tb}, where D is a constant of interaction and $r_{Fe-Tb} = 3.03$ Å [36]; ii) ferromagnetic interaction between Fe–Fe atoms that is one order of magnitude smaller, $D_{Fe-Fe} = -4.805 \cdot 10^{-15}$ erg/r^3_{Fe-Fe} where $r_{Fe-Fe} = 2.5$ Å; iii) interaction between Tb atoms which are magnetized at the interface that is also ferromagnetic, $D_{Tb-Tb} = 3.47 \cdot 10^{-16}$ erg/r^3_{Tb-Tb} where $r_{Tb-Tb} = 3.5$ Å. Interaction between Fe–Fe atoms gives magnetization component in plane of film, while Fe–Tb interaction results in perpendicular magnetization component (Fig. 4). In bare outlines this model was first discussed by Yamauchi et al. [25], where they described four regions in magnetic structure of artificially layered Tb–Fe films: ferrimagnetically coupled Tb–Fe, ferromagnetic Fe, ferromagnetic Tb, and magnetically compensated Tb regions. Later this magnetic structure was improved by Shan and Sellmyer [15], who emphasized that nanoscale layer thickness should be used to show large PMA.
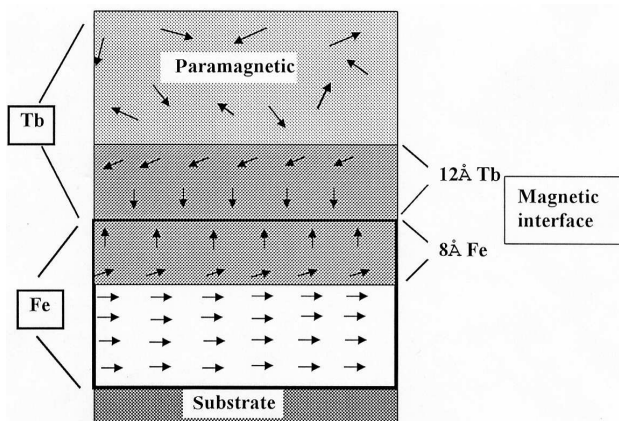

Fig. 4. Model of interlayer interaction in Fe/Tb interface.

Hoffmann and Scherschlicht confirmed this simple model of multilayer system: ferromagnetic Fe (in plane anisotropy)/ferrimagnetic Fe/Tb (perpendicular anisotropy)/paramagnetic Tb/ferrimagnetic Fe/Tb (perpendicular anisotropy)/... [10]. In Fig. 4 we show the detailed magnetic structure of one interface. One can see that if to choose d_{Fe} and d_{Tb} to be equal to «magnetic interface», the in-plane component will tend to minimum.

Magnetic resonance signals for two samples, one for each of two pairs of bilayers which were prepared: i) 8 Fe/12 Tb and 8 Fe/40 Tb (with sharp interface) and ii) 12 Tb/8 Fe and 40 Tb/8 Fe (with rough interface), are shown in Fig. 3,b and c. (Henceforth the number proceeding the chemical symbol refers to the layer thickness in Å). Data for 8 Fe/12 Tb show two resonance lines close to that for control films 8 Fe and 12 Tb. Magnetic resonance signal for the rough 12 Tb/8 Fe interface is significantly different from those of 8 Fe/12 Tb. The Fe signal is absent whereas Tb line is shifted 5 times as compared to that in Fig. 3,b.

Table 1 shows PMOKE data for: 1) control films; 2) bilayers without Au, and 3) trilayers with Au. The in-plane magnetization component, which always presents in the state of nature and characterizes Fe–Fe interactions, is usually observed at high fields (> 1 T) and was well seen for all the samples. The PMOKE signals were not saturated in our experiment up to the maximal field. That is why PMOKE angles at $H = 1.7$ T are given for all the samples to compare.

Besides the high field component the other important features could be seen in PMOKE data for bilayers and trilayers as well. For bilayers we could see two directions of magnetization. The perpendicular magnetization component was always observed at low fields, usually up to 100 mT. This follows from perpendicular geometry which is used

in PMOKE method. We present magnetic fields of saturation and saturated PMOKE angles for bi-layers.

Fig. 5. PMOKE loops for bilayers (a and c) and trilayers (b and d). Only low field component is shown here.

Table 1

Polar magneto-optical Kerr effect data

Sample	Θ_K , min	H_s , mT	Θ_{Ks} , min
8 Fe	11.0		
12 Tb	5.9		
8 Fe/12 Tb	12.1	30	0.75
8 Fe/40 Tb	11.8	240	0.80
12 Tb/8 Fe	9.4	150	0.12
40 Tb/8 Fe	11.3	15	1.0
8 Fe/3 Au/12 Tb	13.6	550	7.3
8 Fe/3 Au/40 Tb	11.8	520	5.5
12 Tb/3 Au/8 Fe	11.8	590	5.5
40 Tb/3 Au/8 Fe	11.7	590	5.3

Θ_K is PMOKE angle at H = 1.7 T (high field component);
H_s is magnetic field of saturation (lower field component);
Θ_{Ks} is PMOKE angle of saturation (lower field component).

The shift of $H_\parallel$ for both lines to the higher fields compared with control films in FMR experiment indicates to the appearance of PMA in bilayers due to Fe-Tb interaction. Magnetization now is out of plane. The PMOKE data (Fig. 5,a,c) support this conclusion. In other words, PMA energy is the measure of Fe — Tb interaction in the interface. Calculation of anisotropy energy based on Eq. (1) for the sharp 8 Fe/12 Tb interface gives value $k_\perp = 0.7 \cdot 10^5$ erg/cm^3. PMOKE data shows a rotation angle of 0.75 min caused by this perpendicular magnetic component.

Having excess of Tb, 8 Fe/40 Tb sample results in almost the same rotation (0.8 min) besides occurring in almost one order more wide field range (240 mT as against 30 mT). This can be interpreted as due to Tb layers with in-plane magnetization in addition to the «magnetic interface» (Fig. 4). For the case of 12 Tb/8 Fe (rough interface) PMOKE angle is only 0.12 min. This is connected with a great variety of angles between Fe and Tb magnetic moments, due to interface roughness, also resulting in the extension of the field range, where this interaction occurs (150 mT as compared to 30 mT for 8 Fe/12 Tb). There is a significant decrease of Fe signal, and no FMR signal was observed (Fig. 3,c). For the bilayers with rough interface ultrathin Fe
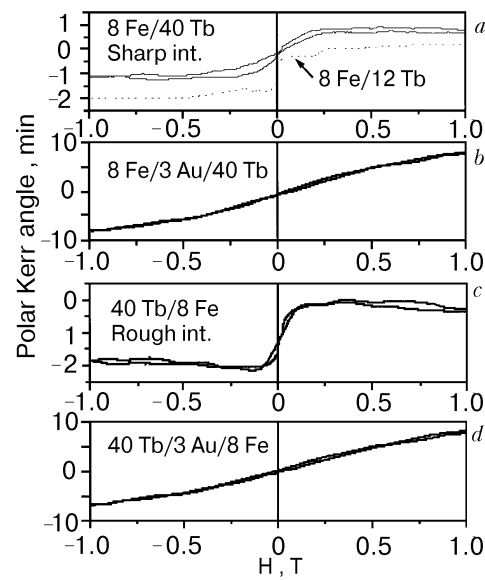
film can be in the superparamagnetic state, leading to disappearance of FMR signal. With more Tb atoms, for 40 Tb/8 Fe bilayer, perpendicular rotation increases significantly (to 1.0 min from 0.12 min for 12 Tb/8 Fe) and also the range of Fe-Tb interaction becomes more narrow (15 mT against 150 mT for 12 Tb/8 Fe, see Table 1). It means that sharp and rough interfaces, having different distribution of atoms need different ratios of Fe and Tb monolayers, participating in the completed «magnetic interface». In other words, the sharp and rough interfaces with the same correspondent layer thicknesses have different effective interface compositions making direct correlation to PMA less straightforward.

Interaction in Fe/Au/Tb trilayers

To further understand the extent of coupling in Fe−Tb system, we introduced one ML of Au at the interface. FMR signals for the trilayers are shown in Fig. 3,d and e: only one FMR signal was observed. It is easily seen that the introduction of Au at the interface causes significant decrease in the resonance field as to the field of 8 Fe/12 Tb bilayer. Now $H_\parallel$ is even smaller than that for 8 Fe film. It means that only one Au ML interposed between Fe and Tb layers was enough to shield the short-range magnetic interactions which resulted in PMA. This is further illustrated in the PMOKE data (Fig. 5). It is natural to suppose that all the magnetic moments in such trilayers are already in the film plane. Though the same PMOKE data for the trilayers, compared with the control Fe film (Fig. 6) show that some small loop of magneti-
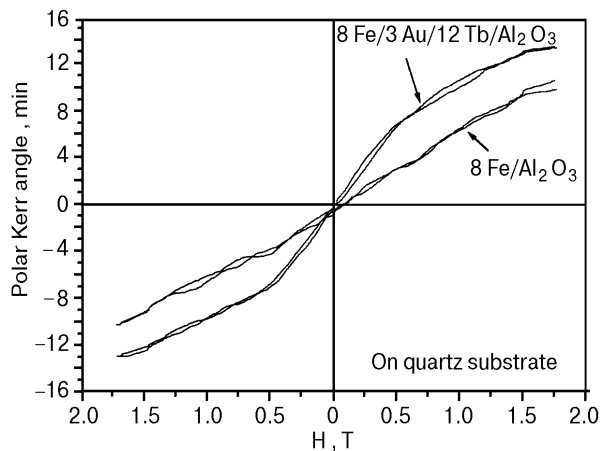
Fig. 6. PMOKE loop for trilayer 8 Å Fe/3 Å Au/12 Å Tb compared with control 8 Å Fe film.

zation with jog at higher fields (500–600 mT) is still present. It means that the angle between Fe and Tb magnetic moments is not zero. Fe and Tb layers still interact via monolayer of Au. The PMOKE angles and fields for the jogs are shown in Table 1 for the different trilayers with Au.

The other characteristic feature is the increase of the total magnetic moment in trilayers (Fig. 6). The same changes of the PMOKE loop shape are observed for both kinds of interface. Small values of Kerr rotation angles and weak FMR signals for the case of rough interface again indicate that Fe magnetic moments are highly disordered there.

So, one ML of Au at the Fe–Tb interface dramatically effects the magnetic interactions, entirely eliminating the short-range exchange between Fe and Tb atoms. Instead a long-range indirect exchange interaction via nonmagnetic Au interlayer is observed leading to the increase in the total magnetic moment. Pan et al. [37] have reported that a magnetic moment is induced in Au by Fe to describe the enhancement of Fe magnetic moment in FeAu alloy film prepared by alternate monatomic deposition. Hoffman also observed that the net magnetic moment for Fe/Au/Tb/Au multilayers is larger than that of pure Fe layers [10]. Magnetic moment induced in Tb still exists. Its orientation as to the Fe-moment is a point of future study.

Conclusions

In summary, using FMR and PMOKE methods we investigated the magnetic interactions in Fe/Tb bilayer system with-sharp as well as rough interfaces. Exchange interaction at Fe-Tb interface induces magnetic moment in thin Tb film that results in two FMR signals, which are shifted from that of free Fe and Tb films. This shift has been attributed to indicate Tb–Fe interaction resulting in a perpendicular anisotropy.

Different distribution of atoms in sharp and rough interfaces with the same correspondent layer thickness leads to different environment for Tb–Fe interactions and hence to different effective compositions.

One momolayer of Au interposed into single Tb–Fe interface of both kinds destroys the «magnetic interface», breaking the short-range interaction. Instead a long-range indirect exchange via nonmagnetic Au interlayer appears.

1. P. Grünberg, R. Schreiber, Y. Pang, M. B. Brodski, and H. Sowers, *Phys. Rev. Lett.* **57**, 2442 (1986).
2. A. Fuβ, S. Demokritov, P. Grünberg, and W. Zinn, *J. Magn. Magn. Mater.* **103**, L221 (1992).
3. J. Unguris, R. J. Celotta, and D. T. Pierce, *J. Magn. Magn. Mater.* **127**, 205 (1993).
4. J. Unguris, R. J. Celotta, and D. T. Pierce, *J. Appl. Phys.* **75**, 6437 (1994).
5. J. Unguris, R. J. Celotta, and D. T. Pierce, *Phys. Rev. Let.* **79**, 2734 (1997).
6. S. N. Okuno and K. Inomata, *Phys. Rev.* **B51**, 6139 (1995).
7. U. Rücker, S. Demokritov, E. Tsymbal, P. Grünberg, and W. Zinn, *J. Appl. Phys.* **78**, 387 (1995).
8. Z. Celinski and B. Heinrich, *J. Magn. Magn. Mater.* **99**, L25 (1991).
9. F. Pan, K. Tao, T. Yang, and B. X. Liu, *Phys. Status Solidi* **A135**, 573 (1993).
10. H. Hoffmann and R. Scherschlicht, *Fesfkörperprobleme*, (Helbig, Vieweg, Braunschweig/Wiesbaden (1998), p. 275.
11. P. Chaudhari, J. J. Cuomo, and R. J. Gambino, *Appl. Phys. Lett.* **22**, 337 (1973).
12. Y. Mimura and N. Imamura, *Appl. Phys. Lett.* **28**, 746 (1976).
13. N. Sato, Y. Aoki, and S. Miyaoka, *IEEE Trans. Magn. MAG-***20**, 1022 (1984).
14. N. Sato, *J. Appl. Phys.* **59**, 2514 (1986).
15. Z. S. Shan and D. J. Sellmyer, *Phys, Rev.* **B42**, 10433 (1990).
16. B.Scholz, R. A. Brand, and W. Keune, *Hyperfine Interactions* **68**, 409 (1991).
17. A. Fnidiki, J. Juraszek, J. Teillet, F. Richomme, and J. P. Lebertois, *J. Magn. Magn. Mater.* **165**, 405 (1997).
18. A. E. Freitag and A. R. Chowdhury, *J. Appl, Phys.* **82**, 5039 (1997).
19. J. Juraszek, A. Fnidiki, and J. Teillet, *J. Appl. Phys.* **84**, 379 (1998).
20. W. S. Kirn, W. Andra, and W. Kleeman, *Phys. Rev.* **B58**, 6346 (1998).

21. W. S. Kirn, W. Kleeman, J. Tappert, and W. Keune, *J. Appl. Phys.* **84**, 4384 (1998).

22. B. Lanchava and H. Hoffman, *J. Magn. Magn. Mater.* **192**, 403 (1999).

23. A. E. Freitag and A. R. Chowdhury, *J. Appl. Phys.* **85**, 4696 (1999).

24. A. E. Freitag and A. R. Chowdhury, *J. Appl. Phys.* **85**, 5756 (1999).

25. K. Yamauchi, K. Habu, and N. Sato, *J. Appl. Phys.* **64**, 5748 (1988).

26. B. Scholz, R. A. Brand, and W. Keune, *Phys. Rev.* **B50**, 2537 (1994).

27. O. M. Kuz'mak, E. V. Shipil, V. I. Shevchenko, and S. Ya. Kharitonski, *Ukr. Fiz. Zh.* **36**, 765 (1991).

28. O. Kuz'mak, A. Pogorily, and V. Shevchenko, *J. Magn. Magn. Mater.* **148**, 36 (1995).

29. E. Shipil and A. Pogorily, *J. Magn. Magn. Mater.* **157/158**, 293 (1996).

30. W. C. Thobum, S. Legvold, and F. H. Spedding, *Phys. Rev.* **112**, 56 (1958).

31. R. F. Soohoo, *Magnetic Thin Films*, Harper and Row, New York (1965).

32. J. R. Fermin, Antonio Azevedo, F. M. de Aguiar, Biao Li, and S. M. Rezende, *J. Appl. Phys.* **85**, 7316 (1999).

33. M. Farle, *Rep. Progr. Phys.* **61**, 755 (1998).

34. B. Heinrich, *Ultrathin Magnetic Structures*, vols. I and II Berlin, Springer (1994).

35. E. Reiger, E. Reinwald, G. Garreau, M. Ernst, M. Zolfl, F. Bensch, S. Bauer, H. Preis, and G. Bayreuther, to be publ. in *J. Appl. Phys.* (MMM'99, paper DQ 02).

36. Y. J. Wang, H. Cai, Q. Tang, K. M. Yang. J. Y. Li, and J. L. Wang, *J. Magn. Magn. Mater.* **66**, 84 (1987).

37. F. Pan, K. Tao, and B. X. Liu, *J. Appl. Phys.* **74**, 1929 (1993).